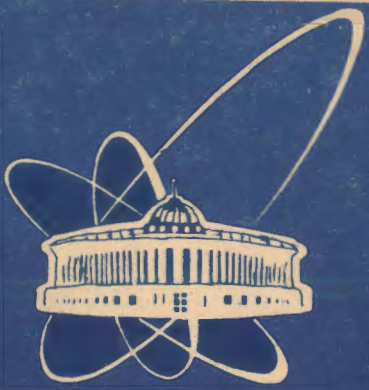

СООБЩЕНИЯ
ОБЪЕДИНЕННОГО
ИНСТИТУТА
ЯДЕРНЫХ
ИССЛЕДОВАНИЙ

Дубна

E9-96-167

S.B.Vorozhtsov, D.V.Altiparmakov*

3D COMPUTER MODEL OF THE VINCY CYCLOTRON MAGNET

*VINCA Institute of Nuclear Sciences, Belgrade, Yugoslavia

1996

1 Design Data

The VINCY Cyclotron is a compact isochronous cyclotron with four straight sectors, designed to accelerate a wide range of ions (≈ 20 μA of 73 MeV deuterons, ≈ 2 μA of 66 MeV protons, heavy ions of lower energy etc).

The description and parameters of the magnetic system under consideration is given in Refs. [1], [2]. Selected set of the most appropriate for the given study parameters is shown in the following Table-1.

Table-1

Diameter of the pole	2000 mm
Maximum extraction radius (for D^-)	860 mm
Spiral angle of the sector	0°
Angular span of the sector	42°
Number of sectors	4
Distance between the hill	51 mm
Distance between the valleys	190 mm
Minimum magnetic gap	31 mm
Number of main coils	2
Maximum power consumption of main coils	110 kW
Maximum magnetic induction at the center	2.1 T
Number of trim coils	10/pole
Maximum power consumption of trim coils	30 kW
Number of harmonic coils	8/pole
Maximum power consumption of harmonic coils	5 kW
Number of the main coil turns/pole	256
Maximum main coil current	920 A
Main coil current at field B(r=0) = 1.84 T	600 A

Various aspects of the system are shown schematically in Fig 1.

Magnetic characteristic [B(H) dependence of induction value "B" on applied field strength "H"] for two possible type of iron were used for the calculations:

- "armco"
- steel 08 [3], [4]

The data on these magnetic materials are presented in Fig. 2

and in the following Tables:

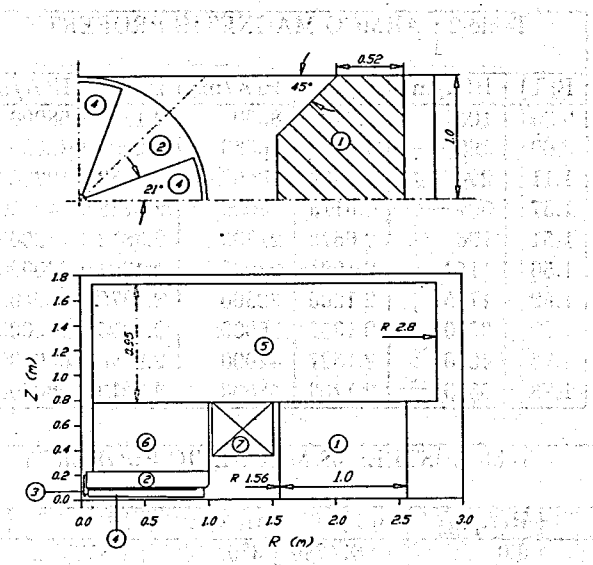

Figure 1: VINCY Cyclotron Magnet Configuration. 1-vertical yoke, 2-pole disk, 3-central plug, 4-sector shims, 5-horizontal yoke, 6-pole, 7-main coil

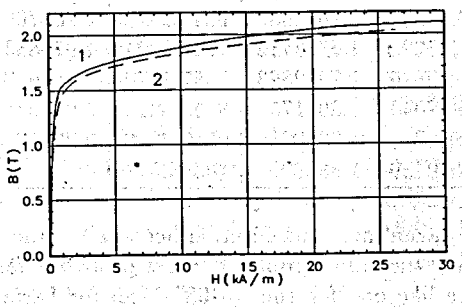

Figure 2: Magnetic property of the cyclotron core steel. 1-"armco", 2-steel 08

Table-2 : ARMCO MAGNETIC PROPERTY

B(T)	H(A/m)	B(T)	H(A/m)	B(T)	H(A/m)
0.30	100	1.84	8000	2.1928	58000
0.69	160	1.898	10500	2.2205	72000
1.11	294	1.9569	13500	2.2682	102000
1.37	501	2.0113	17000	2.3259	140000
1.51	796	2.0673	21800	2.3812	180000
1.56	1154	2.1001	28000	2.4364	220000
1.62	1795	2.1205	32300	2.5370	300000
1.69	3000	2.1352	36000	2.7255	450000
1.73	4000	2.1527	42000	2.9140	600000
1.78	5500	2.1703	48000	3.2910	900000

Table-3: STEEL 08 MAGNETIC PROPERTY

B(T)	H(A/m)	B(T)	H(A/m)	B(T)	H(A/m)
0.0	0.0	1.6671740	3501.4087	1.8533932	11140.846
0.0493226	39.7887	1.6799812	3819.7186	1.8675500	11936.620
0.2221271	79.5774	1.6908231	4138.0285	1.8795473	12732.395
0.4677219	119.3662	1.7016828	4456.3384	1.8918014	13528.170
0.6443858	159.1549	1.7066988	4615.4933	1.9033305	14323.944
0.8664074	238.7324	1.7116702	4774.6483	1.9142617	15119.719
1.0138164	318.3099	1.7165140	4933.8032	1.9250651	15915.494
1.1607398	437.6761	1.7213538	5092.9582	1.9354075	16711.269
1.2340496	517.2536	1.7348483	5570.4230	1.9449435	17507.043
1.2929994	596.8310	1.7556339	6366.1977	1.9545682	18302.818
1.3407906	676.4085	1.7678689	6843.6625	1.9637000	19098.593
1.4248335	875.3522	1.7748412	7161.9724	1.9738631	19894.368
1.4854011	1114.0846	1.7922863	7957.7472	1.9810109	20690.142
1.5676269	1750.7043	1.8091750	8753.5219	2.0132481	23873.241
1.6135324	2387.3241	1.8248878	9549.2966	2.0334833	26260.565
1.6466752	3023.9439	1.8396224	10345.071		

Steel "st-08" was taken into consideration because the measured at the JINR permeability curve for the iron samples of steel proposed for the magnet core fabrication was more like one for the "st-08" than for "armco". This can be well seen in Fig 3. But except "armco" all the other magnetization curves are incomplete and it is not possible to use them in the saturation region where magnetization is $\approx$ constant ($4\pi M \approx 2.16$ T for "armco"). Unfortunately, as it could be seen below this region is of interest for the calculation the magnet in the

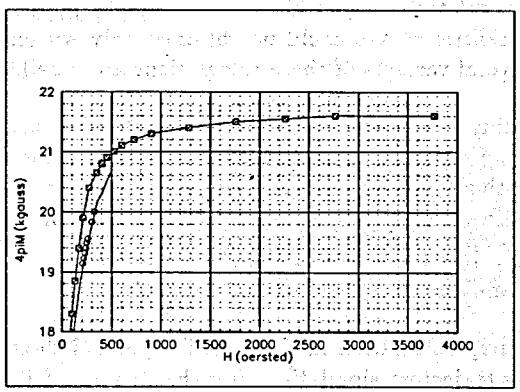

Figure 3: Steel magnetization dependence on applied field strength. Boxes - "armco", Circles - measured for steel 08, solid line - measured in the JINR for the steel sample N1 from the VINCA Institute

working field range. This means one should rely only on the "armco" data for the moment until a new steel sample measurement data, covering also saturation region, be obtainable for the field simulation.

2 Formulation of Problem

- The main goal of the 3D-simulation is a cross check with the 2D calculations (mainly used for the field simulation up to now) to find out some possible limitations of the 2D approach.
  - A construction of the global field map in the median plane is concerned. It is based on one axial symmetrical 2D model and a set of 2D calculations in X-Y geometry (one azimuthal cross section model for every radial point). The former yields the radial distribution of the mean magnetic field, while the latter simulates the azimuthal field variation from the sector shims.
  - Other trouble could arise from the end effects at the very center and at the extraction region of the accelerator. 2D models could give very poor results due to the intrinsic 3D nature of the configuration there.

- There is also a possibility to get a new information on the magnetization curve of the cyclotron magnet for various magnetic permeability of the core. The most realistic curves could be obtained only within 3D model of the magnet. Several variants of these calculations are possible:
  - According to Ref. [1] it is important to get information on "field at the center for different currents of the main coils, without correction coils, and without the sectors. The aim ...is to test the operating range of the main coils" and to compare with the data of the future magnetic field measurements for the magnet.
  - The same but with the sectors in place.

- Stray field map calculation in the region beyond the extraction radius for the particles trajectory simulation after the stripping foil. This information also can be obtained only with 3D magnet model due to intrinsic nature of this field distribution produced by a combination of the round poles, 4 sector shims and yokes of rectangular form and less than 360° azimuthal extension. With the 2D models one can never get the median plane field distribution along the radial lines without the crossing the yokes. This information is needed for the calculation of the transport lines of the extracted beam and to estimate the magnetic field environment for the equipment situated near the magnet (vacuum pumps for example).

- The field contribution of the trim coils obtained with the help of the set of 2D models is also suspected of the possible systematic errors. An overestimation of their contribution could cause serious problem with the ability of the trim coils to produce a necessary isochronous field correction under the given power consumption.

- The same reasoning as above could be applied to the ponderomotive force estimation within 2D models. One should be certain about the magnet structure to sustain these forces when the magnet is on.

3 Calculation Techniques

The following computer codes for performing magnetic field calculations are available for the study:

- 3-dimensional computer simulations of the magnetic field with the help of the program TOSCA [6].

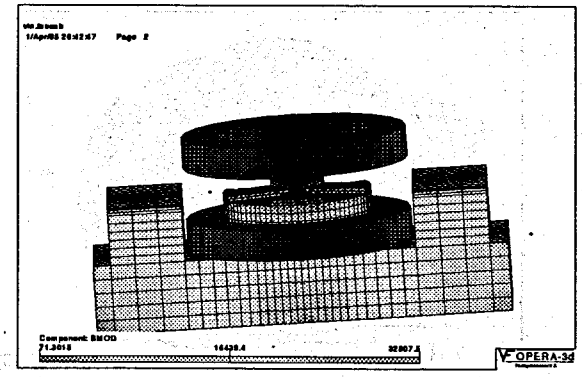

Figure 4: Computer model of the magnet with FE subdivision superimposed on it

- 3-dimensional computer simulations based on the integral technique for calculation of the field outside the iron core: programs MAGSYS [7] at the JINR computers.

4 Computer Model

The first computer model was constructed having in mind the idea to find any problem connected with the 3D structure. The source of the 3D effects are the sector shims and not 360° yokes of rectangular form contrary to the axial symmetry of the poles. To check it one should start with as simple as possible configuration to get quick answer with minimum efforts. If there would be some differences between the 3D and 2D model with the same parameters, one should continue to enlarge and refine the 3D model to get more precise results. The next refined 3D model in the sequence will be enriched with more detailed description of the region around the median plane of the magnet.

This first very simplified 3D computer model of the VINCY cyclotron magnet has been constructed with the help of the VF OPERA-3D - TOSCA package. The magnet configuration with the minimum finite element subdivision (6300 FEs, 27407 nodes for the 2-nd order FEs) is shown in Fig 4.

One can see in this Figure a pair of circular coils, 4-sector shim structure above the pole, horizontal and vertical yokes. For the sake of simplicity the air gap between the sector is constant and equal to 4 cm. Also, the plug is removed.

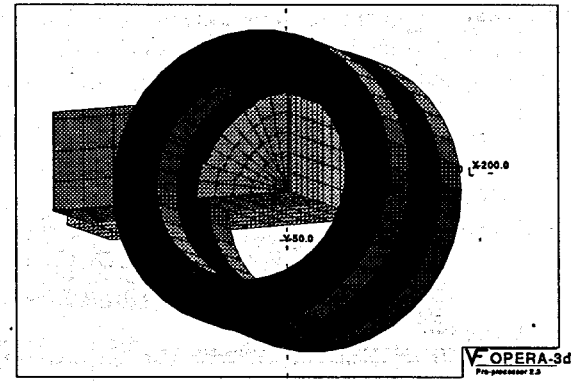

Figure 5: Computer model of the magnet used for the simulation

Sector shims are of constant height and extended to the very center and the end of the pole. No central hole for the ion source is introduced at all.

It is necessary to remark that in the simulation only 1/8 of the magnet iron was taken into consideration. This is due to the existence of the symmetry planes with the positive and negative reflection of the field induction vector. This part of the iron is shown in Fig 5.

5 Simulation Results

5.1 Magnet Magnetization Performance

The data on magnetization curve within above mentioned VINCY cyclotron magnetic model are presented in Fig 6.

There is rather large difference between field levels for "armco" and "st-08" ($\approx$ 0.1 T at J=600 A, which is an operational value for D^- acceleration). The final calculations should be done with an appropriate B(H) curve, that implies a new set of measurements of the cyclotron steel magnetic property for the field strength up to saturation value.

One can also get an impression on the so-called magnet efficiency at the operational point J=600 A. From Fig 6 it is possible to define the ratio of amperturns, "spent" to get the field in the air gap, to the total number of amperturns. In our

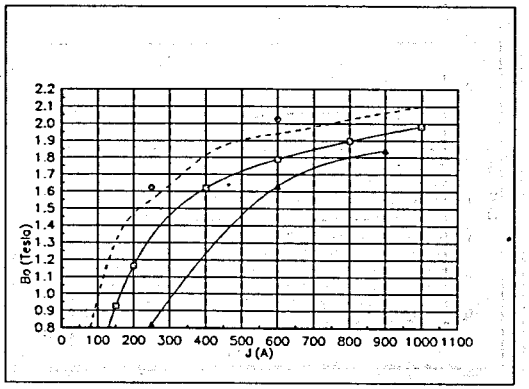

Figure 6: Magnet magnetization curves; circle - "armco"; dash line - "st-08"; box - 2D model, real configuration, "armco"; triangle - no sectors, "armco".

case this ratio is about 40%, that shows rather bad efficiency of the magnet ($\approx$ 60% of the total amperturns are just waisted to overcome magnetic resistance of iron), which leads to relatively large power consumption.

5.2 Field Survey at the Main Coil Current 600 A

Field distributions in the median plane is calculated with the operational coil current of 600 A within the magnetic structure period $\phi = 0^\circ \div 90^\circ$ and presented in Figs. 7, 8 and 9.

Maximum hill value is $\approx$ 2.7 T, that supports the above made statement, concerning the saturation of the sector iron. Radial field dependence over the hill has a waving form with maximums at the interface surfaces of the FE subdivisions. These distortions change their position when the number of FEs is increased in the sector region. This effect shows an artificial nature of the waving. In the valley there is no such a waving due to larger air gap.

To make a comparison of 3D results with the 2D field simulation one should perform this 2D run with the same parameters as in the 3D simplified model. In Fig. 7 one can see that there is rather good agreement between two methods except in the very center and at the magnet edge, where the 3D structure of the field manifests.

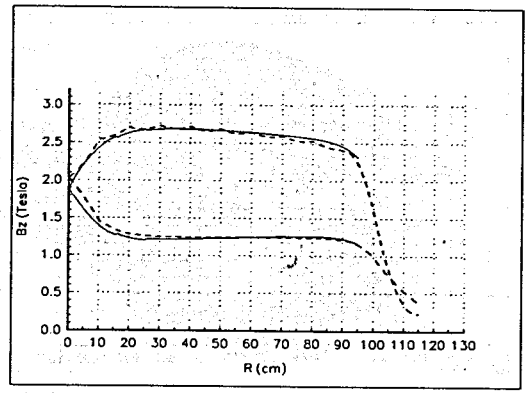

Figure 7: Radial field value dependence. Solid lines - hill field at $\phi = 0°$ and valley field at $\phi = 45°$ for 2D model, dash lines - the same for 3D model.

In Fig. 8 one can see the 3D nature of the magnet stray field distribution beyond the extraction radius. In the radial range 60 cm $\div$ 90 cm the amplitude of the second harmonic is of order 35 mT. The appearance of this harmonic as a result of vertical yokes of the magnet could be detected only within the 3D model.

In Fig. 9 the azimuthal field distributions is shown for three values of radius.

This is worthwhile to compare some experimental data with the VINCY magnet calculation, using 3D simplified model.

The measured azimuthal field of the cyclotron U-200 is shown in Fig. 10. The main magnet parameters of this cyclotron are close to the VINCY one [8] (minimum magnetic gap = 30 mm, diameter of the pole = 2000 mm, number of sectors =4).

One can see that the curve behavior in calculation and in experiment are very similar. The top of the curves in the "hills" are not at all flat and there are some small "holes" at the edges of the "valley". The hill-to-valley field value difference is larger in the VINCY case due to the larger distance between the valleys (190 mm instead of 150 mm for U-200).

The most appropriate way of field analysis would be in terms of field harmonics amplitude and phases. Moreover, only the set of field harmonics matters in the beam dynamics analysis. This will give some kind of smoothing for the obtained

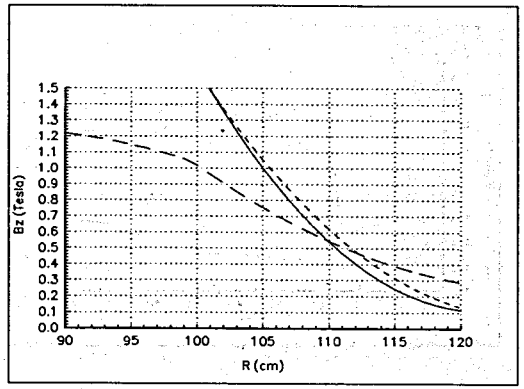

Figure 8: Radial dependencies of stray field. Solid line - hill field at $\phi = 0°$, long dash line - valley field, short dash lines - hill field at $\phi = 90°$.

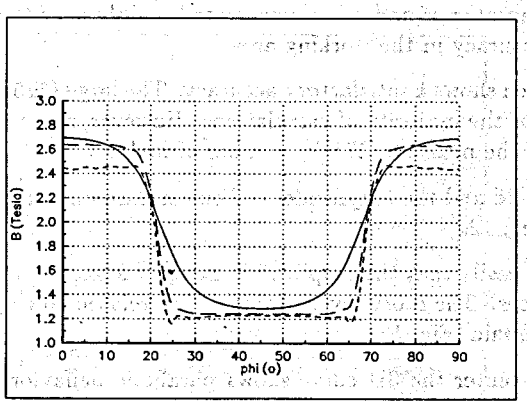

Figure 9: Azimuthal field value dependence, solid line for R = 20 cm, long dash line for R = 60 cm, short dash line for R = 85 cm

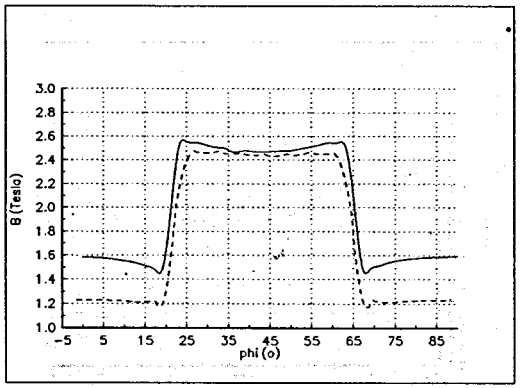

Figure 10: Comparison of the experimental data with the results of the 3D calculations. Solid lines - measurements for the cyclotron U-200, dash lines - calculation for R=85 cm.

median plane field map under the rather coarse grid of the 3D model.

To get feeling of possible errors, related to the finite number of subdivisions, two calculations are carried out with different numbers of grid nodes (Fig. 11). The increased number of nodes is concentrated mainly near the midplane region to get better accuracy in the working area.

This approach shows a satisfactory accuracy. The large (52527) number of grid nodes is used for the majority of calculations. However, some of the calculations were done with the medium (27407) number of nodes.

The mean field and the amplitudes of Fourier harmonics are compared to the 2D results in Fig. 12.

One can see easily that the amplitudes, except the zero order harmonic, agree well in both cases. The most sever problems are related to the difference in the zero order harmonic (Fig. 13).

In the very center the 3D curve shows parabolic behavior within the radial range 0 - 10 cm. Some very small field bump in the same radial range appears. The situation is just opposite in the 2D case: some small hole appears there. To avoid this hole the mesh has to be substantially refined near the axes of symmetry.

One might say that such an error of the order of magnitude of 5% may be acceptable. Unfortunately, it turns out that due to this error, the average field

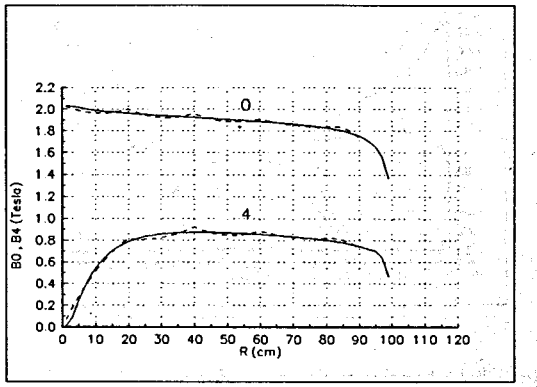

Figure 11: Field Fourier analysis. Dash lines - 8522 nodes, solid lines - 52527 nodes.

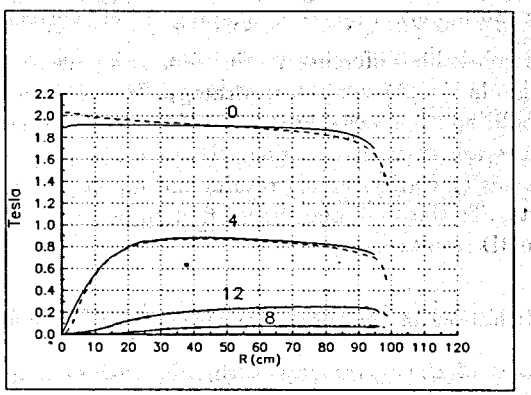

Figure 12: Field Fourier analysis. Solid lines - 2D model, dash lines - 3D model.

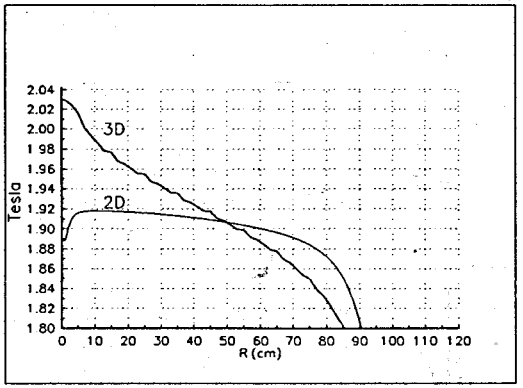

Figure 13: Mean field Fourier radial dependence for 2D model and 3D models.

may differ for 1000 Gauss in central region. The most important difference is in the radial field gradients.

On the other hand the 2D model was used both to determine the isochronous profile of the sectors and to trim the field by concentric correcting coils. In both cases the required accuracy is less than 5 Gauss. Taking into account the above mentioned difference between 2D and 3D models, these calculations become practically useless for an accurate sector shaping or field correction by trim coils.

Due to the remarkable difference in the zero order harmonic, one must do quite some changes in the 2D computing strategy. To avoid the above mentioned problem one should apply a variable stacking factor for the sector region. The preliminary results are very encouraging. However, dealing with such an approach, first one has to clarify the 3D results and moreover to verify them with experimental data. To this end, one should first to perform comparison with as many as possible 3D results.

- Radial distribution for the case without sectors for various currents.
- Computations of the sector case with other values of main coil current (250 A and 900 A).
- The simplified model with the hill to hill gap of 31mm (15.5 mm from median plane) and sector to pole gap of 15mm. It is highly desirable to have these results for three values of main coil current (250, 600 and 900 A).

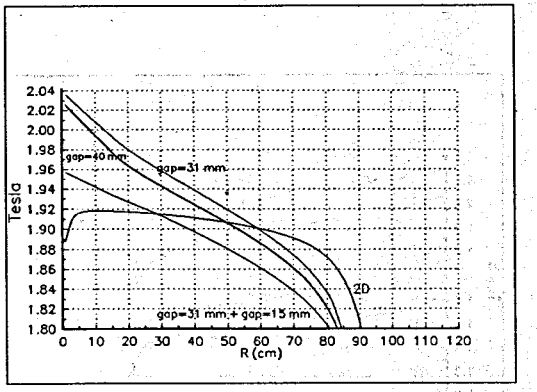

Figure 14: Effect on the mean field of various air gaps.

Having in mind the necessity to get the required isochronous mean magnetic field, the effects of various modifications of the magnetic structure were estimated. The results are shown in Fig 14.

To get rid of the curve waving some smoothing procedure has to be applied to the 3D results. Firstly, the hill-to-hill air gap was reduced from 40 mm to 31 mm. This produced a constant field increase on 150 Gs ÷ 200 Gs. Then the air gap of 15 mm was introduced between the sectors and poles keeping all the other dimensions intact. As a result the negative radial gradient of the field was substantially reduced in absolute value. This modification could be of great help when tailoring the field performance to isochronous one.

Having in mind the 3D results obtained, it is clear that it will be difficult to form an isochronous field by the varying air gap profile only. The angular width of the sector could also be used for this purpose.

5.3 Field Survey at Various Main Coil Current Values

The results of the Fourier analysis for different main coil current are shown in Figs 15 and 16.

In order to check a possible inadequate 2D treatment of the sectors one should get the calculations without sectors (Fig. 17). Comparing 2D and 3D results one can see that there is no such a qualitative difference like in the sector case. In

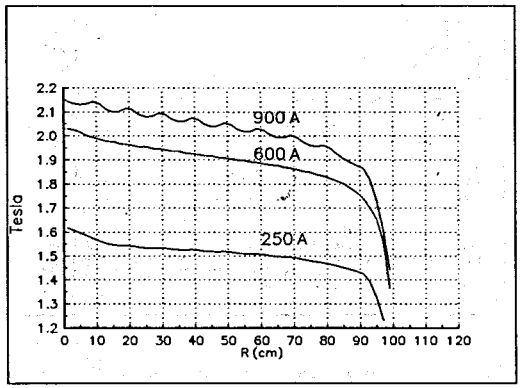

Figure 15: Mean field radial dependencies for different coil currents

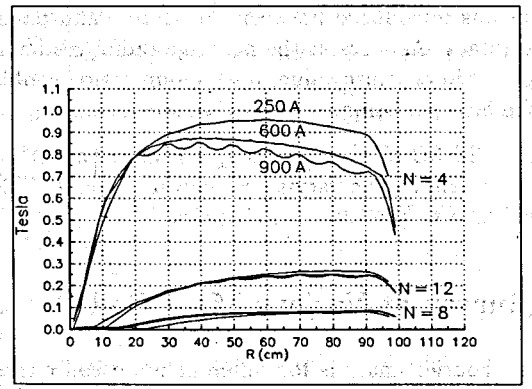

Figure 16: Field Fourier analysis for different coil currents

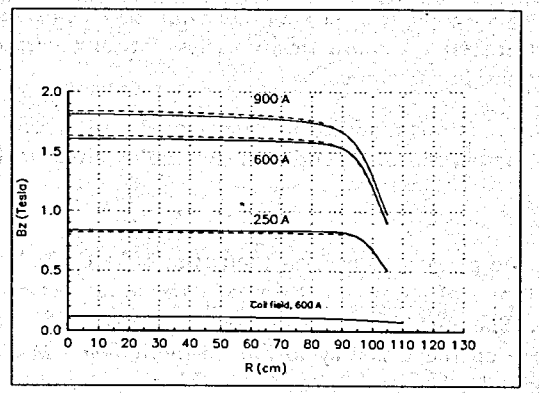

Figure 17: Mean field radial dependencies for different coil currents and no sectors in the system. Solid lines - 2D model, dash lines - 3D model.

the region up to radius of 90 cm, the maximum error of 2D results is equal to 2.2 % , -1.4 % and -1.5 % for the currents of 250, 600 and 900 A, respectively. The qualitative agreement between 2D and 3D results suggests that the source of troubles is possibly in the cylindrization of the sectors.

One can also mention that for the magnet without the sectors and poles at all, the midplane field amounts to 0.24 T at the main coil current equal 600 A. The pure coil field at this current, obtained within the 3D model, is also given in Fig. 17.

6 Conclusion

- Calculations show a rather bad $\approx 40\%$ efficiency of the magnet ($\approx 60\%$ of the total amperturns are just wasted to overcome magnetic resistance of iron), which leads to relatively large power consumption.
- The final calculations should be done with more appropriate B(H) data. That implies a new set of measurements of the magnetic properties of iron for the total field strength up to saturation value.
- Due to the remarkable difference between the 2D and 3D results of the zero order harmonic, one must do quite some changes in the 2D computing strategy.

- The final field simulation can be performed only with the help of 3D method. 2D method should be used only for a preliminary definition of the magnetic system parameters. It is practically useless for an accurate sector shaping or field correction by trim coils.
- The effects of various modifications of magnet structure, that are obtained by the 3D model, can be a good basis for the required field tailoring in the future.

The authors are pleased to express their thanks to Dr.N.A.Morozov for discussing on the topics of study and help with the input data preparing for the field simulation. The authors are also grateful to Prof.I.A.Shelaev for giving us experimental data on the U-200 cyclotron magnetic field. Many thanks also to Mrs.O.V.Lomakina for her help in preparing this manuscript.

References

[1] N.Neskovic et al. TESLA Accelerator Installation, TESLA Report 1/93, Vinca Institute of Nuclear Sciences, Belgrade, 1993.

[2] N.Neskovic et al. TESLA Accelerator Installation. EPAC-Berlin, 24-28th March 1992, p.415.

[3] S.B.Vorozhtsov et al. Permeability Measurements with the Systematic Error Correction by Calculation of Stand Magnets. April 3, 1993. SDC-93-486.

[4] Kukhtin V.V. Measurements of a Magnetization Curve for the Iron Samples. CERN/EP/NA-4 Note, August 21, 1984.

[5] Kalinichenko V.V. Private Communication.

[6] Tosca User Guide. Version 6.3. 1993.

[7] Borisovskaja Z.V., et al., JINR, B1-9-85-232, Dubna, 1985.

[8] Shelaev I.A. Thesis. Dubna 1970.